Analysis of MTMs in NSTX: Progress Report

Joel Larakers, Mate Lampert, David Hatch, Ahmed Diallo

May 2022

1 Introduction

The microtearing mode (MTM) is an electromagnetic mode driven by the electron temperature gradient. It occurs about rational surfaces and causes radial magnetic fluctuations. It has been theorized to be a component of the anomalous electron heat transport and bands of magnetic fluctuations that are present in NSTX. In both linear and nonlinear NSTX gyrokinetic simulations, MTMs are commonly found[1]. They have even been shown to provide the necessary nonlinear heat flux to provide power balance[1]

The gyrokinetic simulations provide good evidence that MTMs are present in NSTX. Our work described here seeks to provide an additional line of evidence that MTMs are active. We do this by applying reduced models of the MTM and comparing the results with experimental data. In the process, we seek to understand the nature of MTMs in NSTX.

We seek an independent line of evidence by directly comparing reduced MTM models to experimental data of magnetic fluctuations taken from the wall of the vessel. The goal being if we predict MTMs in our models then we should also see their signatures in experiment. [1] We should also expect that the frequency of these magnetic fluctuations should be correlated with the evolution of the electron profiles. [2] The main goal of this work is to get mode number and frequency matching between the observed magnetic fluctuations and those predicted by our reduced models or gyrokinetic simulations.

[1] if the MTM mode width is large enough to interact with magnetic pick-up coils on the walls of the vessel. Note an estimate of this criteria is given in the appendix

[2] since the real frequency of the MTM is approximately $\omega \approx \omega_{*n} + \omega_{*T}$. Where $\omega_{*T} = ck_y T/eBL_T$ and $\omega_{*n} = ck_y T/eBL_n$ are the electron drift frequencies and L_n and L_T are length scales describing the characteristic variation of the electron density and temperature.

2 Methodology

The microtearing mode is a complex excitation which depends on a large set of parameters. The essential characteristics identify the mode, [3] however the mode's stability and other features can broadly vary for changes in the parameter space. We have primarily focused our work so far on analyzing NSTX for conventional slab MTMs. More exotic MTMs that depend upon trapped particles and/or magnetic drifts are studied using gyrokinetic simulations. [4]

In this research we have applied three different levels of MTM stability analysis: (i) Intuition based off basic MTM parameters (ii) Applying a sophisticated slab model eigenvalue solver, (iii) Gyrokinetic simulations. Most of the research progress and problems we are currently facing can be understood solely from the basic MTM parameters.

Magnetic fluctuation spectrograms from many NSTX discharges are readily available. We have used the spectrograms as a first sorting tool to determine which discharges are of interest. The sign of the mode frequency (ie. the propagation direction) and the toroidal mode number can also be determined from the fluctuation data. The pick up coils are only sensitive to about n=8. It is known that the magnetic pick up coils have difficulty picking up higher mode number fluctuations.

2.1 Basic MTM Parameters

In this section, we will review four robust properties of the MTM that we have applied in our analysis. These properties allow us to swiftly garner intuition as to whether or not to expect an MTM.

1. $\omega \approx \omega_{*n} + \omega_{*T}$
2. For slab MTM to be unstable $\nu/\omega \sim 1$
3. For slab MTM to be unstable $\hat{\beta} = \beta/(L_T/L_s)^2 >> 1$
4. MTMs are most unstable at the peak in ω_*

2.1.1 Real Frequency

Perhaps the most robust feature of the MTM is its real frequency which is estimated by

$$\omega \approx \omega_{*n} + \omega_{*T}.$$

Since ω_* is proportional to k_y this frequency is also proportional to the mode number of the fluctuation. This formula provides us with a useful benchmark to determine if an observed mode is an MTM. It also provides-perhaps more

[3] electromagnetic, tearing parity about rational surfaces, driven by electron temperature gradients.

[4] We have attempted to improve our slab model to include magnetic drifts. Please see the Appendix.

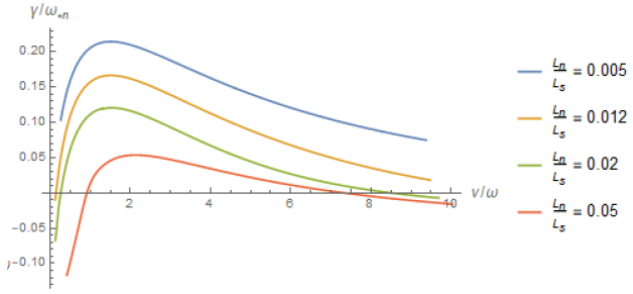

Figure 1: Here we display the growth rate of the MTM as a function of ν/ω. Here we have also varied L_n/L_s, the magnetic shear. $\eta = 1.0$ and $\beta = 0.01$

importantly-an estimate of the gap between successive mode numbers. This frequency gap is given by:

$$\Delta\omega = \omega_{n+1} - \omega_n = \frac{q}{a}\frac{cT}{eBL_p}$$

Where q is the safety factor and a is the minor radius. We see that this difference is independent of mode number. Thus in experiment if a set of successive MTMs are unstable, we would expect to see equally spaced bands of fluctuations with a gap estimated by $\Delta\omega$. This turns out to be a useful tool for quickly analyzing magnetic spectrograms. This results lies on the assumption that rational surfaces are close enough radially that the local parameters: q, L_n, L_T, T_e do not vary greatly.

2.1.2 The parameter ν/ω

The slab MTM has a nonmonotonic dependence of collisionality. It is stable when $\nu/\omega << 1$, unstable when $\nu/\omega \sim 1$, and stable again when $\nu/\omega >> 1$. Figure 1 displays this result. Since ω is roughly linearly proportional to the mode number, this feature can be applied to roughly determine the interval of mode numbers that will be unstable.

2.1.3 The parameter $\hat{\beta}$

The microtearing mode is driven unstable the electron temperature gradient $1/L_T$, is stabilized by magnetic shear $1/L_s$, and since it is electromagnetic more unstable at large β. The parameter $\hat{\beta} = \beta/(L_T/L_s($^2 combines these features into a single useful parameter. When $\hat{\beta} >> 1$, we expect the MTM to be unstable.[5]

[5]The MTM is a complex mode and can be unstable for $\hat{\beta} \sim 1$, although this branch is not as robust. See Chapter 5 of [2]

2.1.4 Global effects

Strong profile variation can also effect the mode if the mode width is the same order of the profile variation. In standard aspect ratio tokamaks these global effects can stabilize MTMs that otherwise would have been unstable [3, 5, 6]. The important feature that was discovered is that MTM in the pedestal are most unstable at the peak in ω_*.

In our fluctuation analysis we will apply these zeroth order features. For analytical intuition, we will also write down a simple MTM dispersion relation, that is derived in the high collisionality and high $\hat{\beta}$ limit[2, 4]. This dispersion is given by

$$\omega = \omega_{*n} + \omega_{*T}\big(1 + 0.8i(\omega/\nu)\big) - i0.85\omega_{*n}\left(\frac{\omega - \omega_{*n}}{\hat{\beta}\omega}\right)^{1/2}$$

2.2 Slab Model

The most broadly studied parameter space of the MTM has been the MTM in slab geometry. The slab geometry is approximately valid in the pedestal region where gradient length scales dominate over the machine's geometrical parameters. Here we apply a sophisticated slab model code and intuition to analyze MTMs in different NSTX discharges. This model has been described in the following papers [3, 6]

The slab model of the MTM is limited in very real ways, and serves best as an analytical benchmarking tool. It also neglects a variety of FLR effects. It is of interest to improve the model. We have looked into adding magnetic drifts into the model. Progress on this work is shown in the appendix.

2.3 Gyrokinetic Simulations

We also have at our disposal advanced gyrokinetic simulations which can capture physics that is left out in the slab model.

3 Results

We have analyzed a large set of magnetic spectrograms from NSTX discharges and parameters from EFITS of these discharges. From these discharges we have selected two to study in great depth. The first discharge is 139034 and the second discharge is 132588. 132588 is a highly lithiated discharge with a wide pedestal while 139034 is a more standard NSTX discharge with a narrow pedestal. The characteristics of these two discharges are very distinct, and thus different conclusions on MTM prevalence are made.

To analyze a discharge, we begin by plotting the important MTM parameters and investigating the magnetics. An example of these plots is shown in Figure 2. The parameters are plotted using the toroidal mode number $n = 1$, since

ω_{*T} can be written as

$$\omega_{*T} = \frac{nq}{a}\frac{cT}{eBL_T},$$

and similarly for ω_{*n}. The plots can easily be converted by either multiplying or dividing by toroidal mode number of interest. These plots provide a simple process to predict the mode numbers that MTM will be active.

We begin by determining the rough location of the peak in either ω_* or $\hat{\beta}$[6]. Next we investigate the $n = 1$ collisionality plot at this radial location. For the MTM to maximally unstable $\nu/\omega \sim 1$, thus we can estimate the toroidal mode number where this criteria is satisfied. With this toroidal mode number we can multiply the green curve in the bottom plot to determine the expected frequency observed in experiment.

We can then follow up this simple analysis by comparing these predicted mode numbers and frequencies with the magnetic spectrograms. These estimates can be further verified by carrying out slab model calculations and gyrokinetic simulations.

3.1 Discharge 139034

The magnetic spectrogram and mode numbers for each fluctuation band is displayed in Figure 3. The magnetic spectrogram displays bands of fluctuations between ELM cycles.

The MTM parameters for this shot are shown in Figure 2. Using the process outlined above, we can predict the unstable MTM mode numbers. The rough radial location of the peak in $\hat{\beta}/\omega_*$ is $\rho_t = 0.94$. At $\rho_t = 0.94$ and for $n = 1$ the collisionality plot indicates that $\nu/\omega_{n=1} \approx 30$. This ratio is far too large for low mode numbers, and thus we expect MTMs to appear at largish mode numbers in a rough range from $n = 8 - 20$. The magnetic spectrogram should thus show equally spaced bands of fluctuations with frequencies around $\omega \sim 120 - 300$ kHz and spacing approximately equal to 15 kHz.

Unfortunately the magnetic diagnostics have difficulty picking up high toroidal mode number fluctuations. We do not oberserve these frequency bands in experiment. By inspecting Figure 3, we see that there are no fluctuation bands present in the 120-300 kHz band. The bands at lower frequency can also not be attributed to MTMs since they rotate in the ion direction. The sources of these fluctuations is a current topic of research.

We have analyzed roughly 5 other narrow pedestal NSTX discharges using this same procedure and found similar results. Our final conclusion is given below.

Conclusion. *Due to the high collisionality in 139034, we only expect MTMs of mode number $n \sim 8-20$ to be active. These mode numbers are much too high to be resolved by magnetics and thus will not be observed in magnetic spectrograms. A new diagnostic is necessary to experimentally verify high mode number MTMs.*

[6] They typically lie near one another

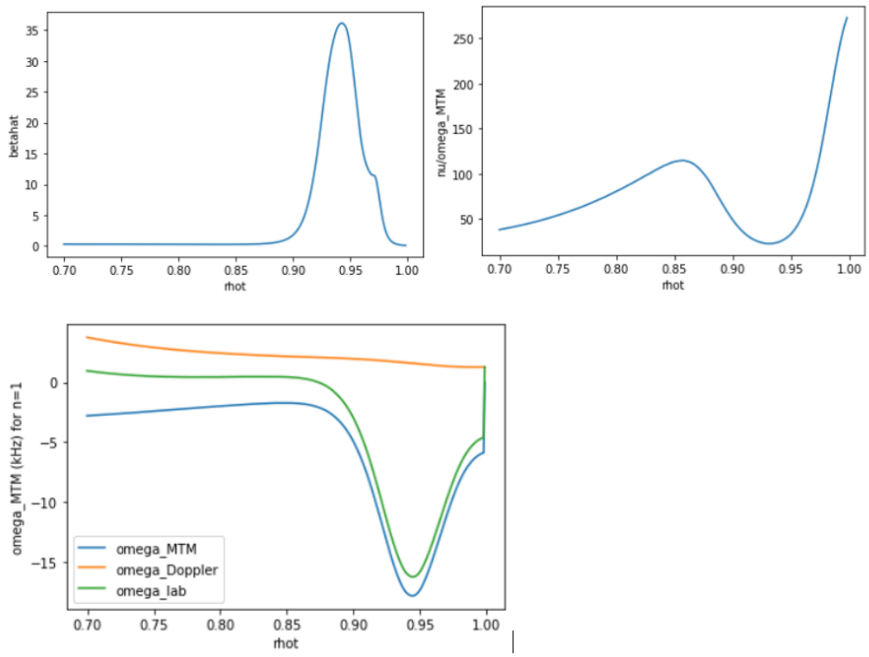

Figure 2: Top left: This displays the parameter $\hat{\beta}$ which should be large for MTMs, Top right: This displays the important collisionality ratio ν/ω for $n = 1$. We see that for $n = 1$ the collisionality is far too high and we expect the mode to be stable. This plot can be converted to higher n by dividing by n. Bottom: This plot displays the expected real frequency of the mode in the lab frame (green). The blue curve is the MTM frequency in the plasma frame and the orange is the doppler shift. Again this is for $n = 1$. The negative frequency indicates that the mode rotates in the electron direction.

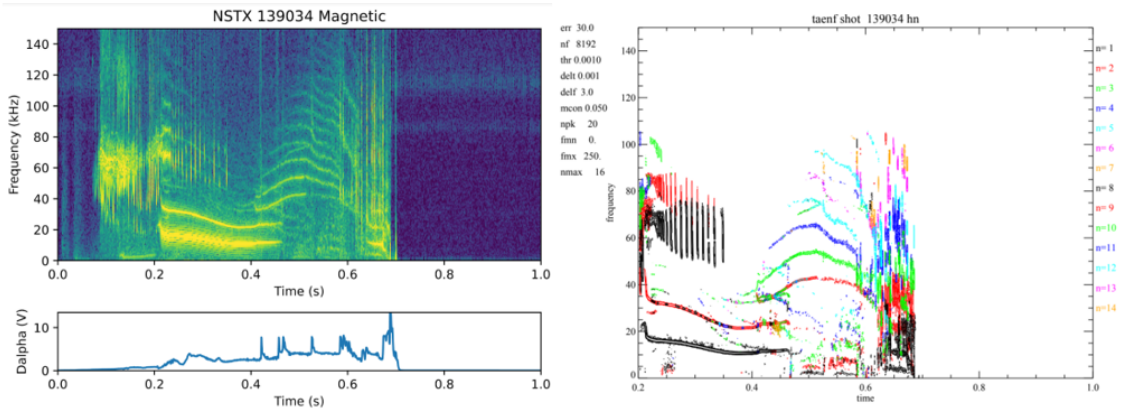

Figure 3: Left: Magnetic spectrogram from 139034. The verticle lines in the spectrogram and the Dalpha signal identifies ELMs. We are seeking to understand the source of the bands of fluctuations. Right: Using magnetic data the toroidal mode numbers and propagation direction of the mode can be determined. Positive frequency indicates that all of these modes rotate in the ion direction.

3.1.1 Slab Model Analysis

The high mode number MTMs will not be accurate with the slab model. Since the slab model neglects a variety of FLR effects. Gyrokinetic simulations are optimal for high mode number MTMs.

3.1.2 Gyrokinetic Simulations

3.2 Discharge 132588

We now proceed to analyze the discharge 132588 using the same procedure. This discharge is known to have be a highly lithiated discharge with a wide pedestal and large confinement time[7].

The parameters for 132588 are shown in Figure 4. We see that the radial location of the peak in ω_* is roughly $\rho_t = 0.8$ and that the collisionality at this location is roughly $\nu/\omega \sim 5$ for $n = 1$. This implies that we should observe low mode number MTMs $n = 2 - 8$ in the magnetic spectrograms. Using these results we can construct a table of predictions for the observed mode numbers and frequencies. We also understand that since low mode number rational surfaces are sparse, we may observe mode skipping due to offset stabilization.

We now compare these predictions with the magnetic spectrogram. This is shown in Figure 5. The spectrogram displays the same mode numbers predicted to be unstable above. $n = 2$ through $n = 5$ are observed in the spectrogram, however the frequency is the ion direction. The mode spacing is near enough to be reasonable within some degree of uncertainty and approximation. The main

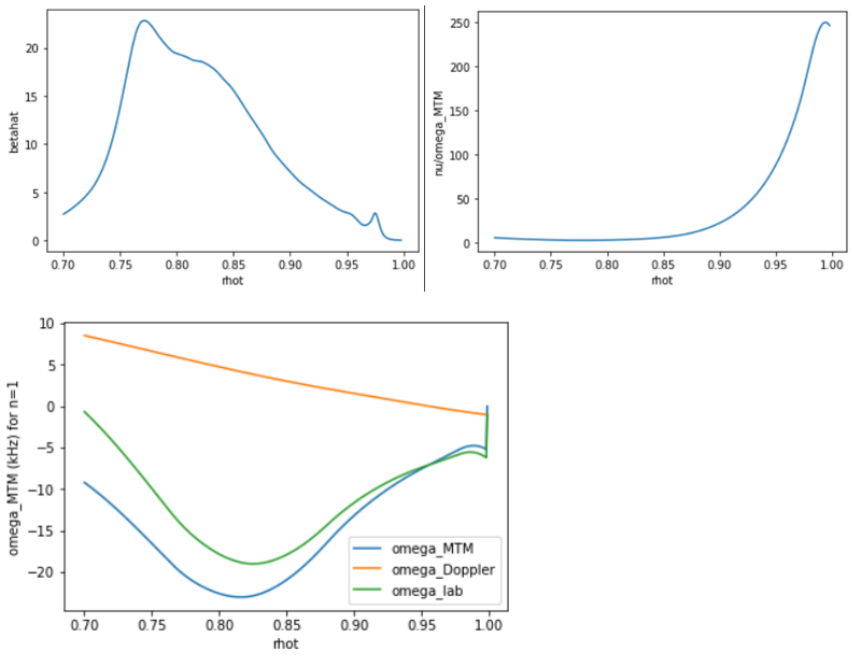

Figure 4: Top left: This displays the parameter $\hat{\beta}$ which should be large for MTMs, Top right: This displays the important collisionality ratio ν/ω for $n = 1$. We see that for $n = 1$ the collisionality is far too high and we expect the mode to be stable. This plot can be converted to higher n by dividing by n. Bottom: This plot displays the expected real frequency of the mode in the lab frame (green). The blue curve is the MTM frequency in the plasma frame and the orange is the doppler shift. Again this is for $n = 1$. The negative frequency indicates that the mode rotates in the electron direction.

Mode number	Frequency
n=2	-34 kHz
n=3	-51 kHz
n=4	-68 kHz
n=5	-85 kHz
n=6	-102 kHz

Table 1: Predicted MTM mode numbers and frequencies

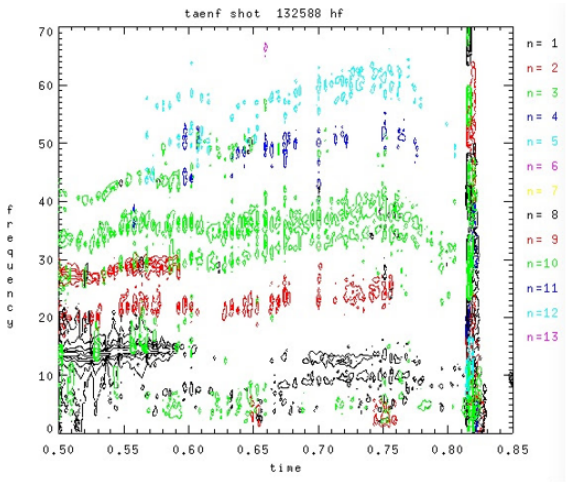

Figure 5: Magnetic spectrogram and mode numbers from 132588 during an inter ELM cycle. Positive frequency indicates that all of these modes rotate in the ion direction. No modes were found to propagate in the electron direction

Mode number	Unstable?	Dispersion	Doppler	Predicted
n=2	Unstable	-39 kHz	7 kHz	-30 kHz
n=3	Unstable	-55 kHz	14 kHz	-41 kHz
n=4	Stable	-70 kHz	18 kHz	-53 kHz
n=5	Stable	-86 kHz	21 kHz	-64 kHz

Table 2: Predicted MTM frequencies from the Slab eigenvalue solver

issue is the incorrect propogation direction. This discrepency is a current topic of research and analysis.

We have studied one other Lithiated shot and found similar predictions. The lower collisionality combined with the wider pedestals provide a better case for low mode number MTMs to be active. More Lithium cases are being compiled to study this further. Our current conclusion thus far is given below.

Conclusion. *Lithium discharges with their wider pedestals and lower collisionality are predicted to have active low mode number MTMs. Magnetic spectrograms from discharge 132588 displays the low mode number excitation, but they rotate in the wrong direction. This discrepancy is a current topic of research*

3.2.1 Slab Model

We have further analyzed this discharge using the slab MTM eigenvalue solver. Table 2 below shows the results.

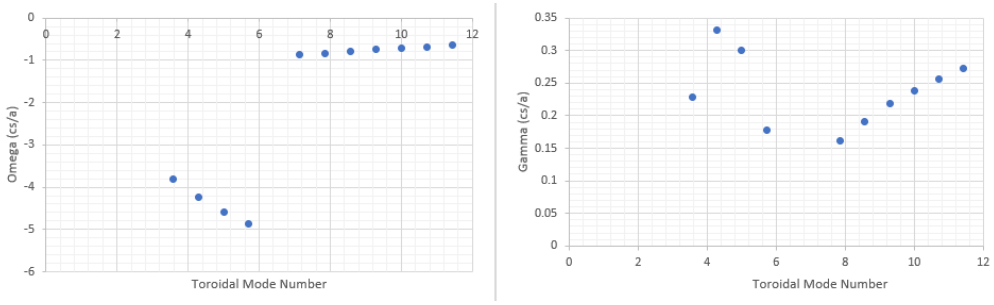

Figure 6: Left: Real frequency of the mode as a function of toroidal mode number. We see that there is a mode transition at n=6. The low mode numbers match the MTM predictions: electron direction, proportional to mode number. Right: The growth rate as a function of mode number. The low mode numbers have the characteristic nonmonotonic dependence which is caused by the ν/ω dependence.

3.2.2 Gyrokinetic simulations

We have performed gyrokinetic simulations at the radial location $\rho = 0.825$ near the peak in ω_*, to solidify our low mode number MTM predictions. We have successfully found MTMs at mode numbers $n = 4$, $n = 5$, and $n = 6$. We are currently battling numerical issues that appear at $n = 2$ and $n = 3$. Plots of the growth rate and frequency are shown in Figure 6. A characteristic eigenfunction is also shown in Figure 7.

4 Conclusions

Here we have presented a methodology for determining if microtearing mode magnetic fluctuations are present in experimental measurements. This thrust would serve as independent evidence that MTMs are active in NSTX.

This methodology is limited, in that experimental diagnostics cannot resolve high mode number excitations and fluctuations that do not extend out to the edge of the device. We have also primarily focused on conventional aspects of MTM theory. The variety of physical effects in NSTX could in principle effect these aspects. It is of our assumption that the robust features of the MTM should be unchanged.

We have applied this methodology to many narrow pedestal discharges and a couple of Lithium (wide pedestal) discharges. In this document, we have described in detail an analysis of two discharges 139034 (narrow pedestal) and 132588 (wide pedestal). Our main conclusions from these two discharges are repeated below.

Conclusion. *Due to the high collisionality in 139034, we only expect MTMs of mode number* $n \sim 8-20$ *to be active. These mode numbers are much too high to*

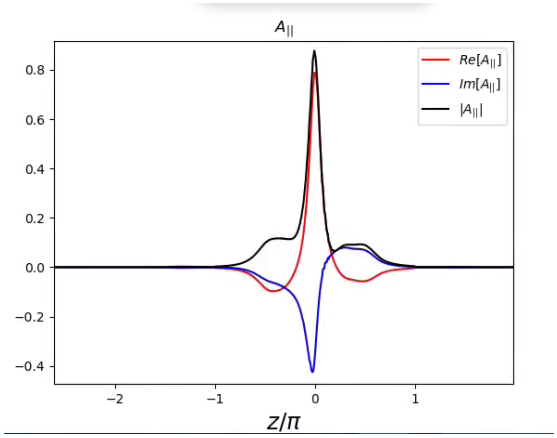

Figure 7: Eigenfunction of a GENE simulation of for $n \approx 4$. We see tearing parity a feature of the MTM.

be resolved by magnetics and thus will not be observed in magnetic spectrograms. A new diagnostic is necessary to experimentally verify high mode number MTMs.

Conclusion. *Lithium discharges with their wider pedestals and lower collisionality are predicted to have active low mode number MTMs. Magnetic spectrograms from discharge 132588 displays the low mode number excitation, but they rotate in the wrong direction. This discrepancy is a current topic of research*

5 Future Work

It is fair to say that this work does not provide sufficient evidence that MTMs are producing magnetic fluctuations. There is much work left to answer this question. The most optimistic avenue is to continue investigating more Lithium (wide pedestal) discharges using the same methodology.

From the few Lithium cases that we have studied, their parameters align well within the MTM instability window. It would be interesting to see if these features from these couple of discharges are universal in wide pedestals.

In addition to this avenue there remains a few other discrepancies and details that needed to be sorted out. I have enumerated these avenues below:

1. Analyze more Lithium discharges using same methodology (already mentioned)

2. Verify the experimentally measured propagation direction. Determine if the Doppler shift or direction calculation is valid. Within uncertainty can this be made consistent with theory

3. Continue performing gyrokinetic simulation on 132588 to verify the existence of MTMs at n=2 and n=3

4. Continue performing gyrokinetic simulations for 139034 or other narrow pedestal shots and look for high mode number MTMs. The equilibrium may need to be modified within uncertainty

5. Are there other diagnostics that could be applied to measure high mode number MTMs?

6 Acknowledgements

We'd like to thank Erik Fredrickson, who has made his tools for analyzing magnetic fluctuations readily available.

7 Appendix

7.1 Including Magnetic Drifts

7.1.1 Motivation

Spherical tokamaks (STs) have magnetic drift frequencies that are comparable to ω_* even in the pedestal region. Gyrokinetic simulations indicate that magnetic curvature and trapped particles play a role in MTM stability. Here we analyze the simplest physical extension which allows us to study the effect of magnetic drifts on the mode. Trapped particles effects are left for future analysis.

7.1.2 Geometry

Let's consider an axisymmetric magnetic field in cylindrical geometry. The magnetic field forms concentric cylindrical flux surfaces with a field given by.

$$\mathbf{B}(r) = B_\phi(r)\big(\hat{\phi} + \alpha(r)\hat{z}\big)$$

Where $\alpha(r) = B_z/B_\phi$, r is the radial coordinate, ϕ is the azimuthal, and z is along the axis. The magnetic field in the ϕ direction is produced by a central current along the z axis while B_z is produced via plasma current.

This configuration has a magnetic curvature given by

$$\kappa = \hat{b}\cdot\nabla\hat{b} = -\frac{1}{r}\left(\frac{1}{1+\alpha^2}\right)\hat{r}$$

and a gradient given by

$$\nabla B_0 = \frac{\partial B_0}{\partial r}\hat{r} = B_0\left(\frac{1}{L_B} + \left(\frac{\alpha^2}{1+\alpha^2}\right)\frac{1}{L_\alpha}\right)\hat{r}$$

Here $B_0 = B_\phi\sqrt{1+\alpha^2}$, $1/L_B = (\ln B_\phi)'$, and $1/L_\alpha = (\ln\alpha)'$.

Thus a plasma embedded in this geometry will have equilibrium magnetic drifts. Our goal in this calculation is to include these drifts into the conventional

slab microtearing mode theory. We hope to find interesting modifications to the dispersion of the mode.

We will perturb the system with a vector defined as

$$\mathbf{k} = \frac{m}{r}\hat{\theta} - \frac{m}{\alpha(r_0)r_0}\hat{z}$$

Such that

$$\mathbf{k}\cdot\mathbf{b}\Big|_{r=r_0} = 0$$

Here m is an integer and r_0 is the location of a rational surface of interest.

7.1.3 Kinetic Equation

We begin with the drift kinetic equation for electrons which is given by

$$\frac{\partial f}{\partial t} + \big(v_\parallel \hat{b} + \mathbf{V}_E + \mathbf{V}_D\big)\cdot\nabla f + \Big(\mu\frac{\partial B}{\partial t} + e\big(v_\parallel\hat{b} + \mathbf{V}_E + \mathbf{V}_D\big)\cdot\mathbf{E}\Big)\frac{\partial f}{\partial w} = C(f) \quad (1)$$

Here w is the particle kinetic energy $w = mv^2/2$. The drift velocities are given by

$$\begin{aligned} v_\parallel &= \hat{b}\cdot\mathbf{v} \\ \mathbf{V}_E &= \frac{c\mathbf{E}\times\mathbf{B}}{B^2} \\ \mathbf{V}_D &= \frac{1}{\Omega}\hat{b}\times\Big(\frac{\mu}{m}\nabla B + v_\parallel^2\kappa + v_\parallel\frac{\partial\mathbf{B}}{\partial t}\Big) \end{aligned}$$

We now linearize this equation about the following equilibrium

$$f_0 = \frac{n(r)}{\pi^{3/2}v_e^3(r)}\exp\big(-\frac{mv^2}{2T(r)}\big)$$

where $v_e = \sqrt{2T(r)/m_e}$. We now linearize

$$-i\omega f_1 + ik_\parallel v_\parallel f_1 - C(f_1) + \big(\mathbf{V}_{D0}\cdot\nabla\big)f_1 = -\big(v_\parallel\hat{b}_1 + \mathbf{V}_{E1} + \mathbf{V}_{D1}\big)\cdot\hat{r}\frac{\partial f_0}{\partial r} + ev_\parallel E_\parallel\frac{\partial f_0}{\partial w} + \Big(e\mathbf{V}_{D0}\cdot\mathbf{E} + \mu\frac{\partial B_1}{\partial t}\Big)\frac{\partial f_0}{\partial w} \quad (2)$$

The terms involving $\mathbf{V}_{D0}$ and $\mathbf{V}_{D1}$ are all new terms to the conventional theory.

7.1.4 New Terms

Let's first consider computing $\big(\mathbf{V}_{D0}\cdot\nabla\big)f_1$. The equilibrium magnetic drift is given by.

$$\mathbf{V}_{D0} = \frac{1}{\Omega}\left(\frac{v_\perp^2}{2}\big(\frac{1}{L_B} - \frac{\alpha}{1+\alpha^2}\frac{1}{L_\alpha}\big) - v_\parallel^2\frac{1}{r}\frac{1}{1+\alpha^2}\right)\hat{r}\times\hat{b}$$

Thus

$$\big(\mathbf{V}_{D0}\cdot\nabla\big)f_1 = \frac{1}{\Omega}\left(\frac{v_\perp^2}{2}\big(\frac{1}{L_B} - \frac{\alpha}{1+\alpha^2}\frac{1}{L_\alpha}\big) - v_\parallel^2\frac{1}{r}\frac{1}{1+\alpha^2}\right)ikf_1$$

For simplicity we assume $|\alpha| << 1$ and that $L_B \sim r$. This gives.

$$\big(\mathbf{V}_{D0}\cdot\nabla\big)f_1 = i\omega_B s^2(1+\zeta^2)f_1$$

Where $\omega_B = ckT/(eBL_B)$ and we have defined dimensionless velocity space variables: $s = v/v_e$ and $\zeta = v_\parallel/v$.

We now investigate the second term which involves the perturbed magnetic drift. The perturbed magnetic drift is given by.

$$V_{D1}\cdot\hat{r} = \frac{1}{\Omega}\Big(\frac{v_\perp^2}{2}X_{\nabla B} + v_\parallel^2 X_\kappa\Big)$$

Where

$$X_{\nabla B} = \frac{im\big(r + r_0\alpha(r)\alpha(r_0)\big)\big(-\alpha(r) + r\alpha'(r)\big)}{r^2 r_0 B_\phi(r)\alpha(r_0)\big(1+\alpha(r_0)^2\big)^2}A_\parallel(r)$$

and

$$X_\kappa = \frac{im\big(r + r_0\alpha(r)\alpha(r_0)\big)\big(1+\alpha(r)^2+\sqrt{1+\alpha(r_0)^2}\big)\big(-\alpha(r) + r\alpha'(r)\big)}{r^2 r_0 B_\phi(r)\alpha(r_0)\big(1+\alpha(r_0)^2\big)^2}A_\parallel(r)$$

We can expand these terms about $r = r_0$.

7.1.5 Final Form

This can be put into more conventional form. Here we define $s = v/v_e$ $\zeta = v_\parallel/v$.

$$\Big(-i\omega + ik_\parallel v_e s\zeta + \omega_B s^2(1+\zeta^2)\Big)f_1 + C(f_1) = -\big(v_\parallel\hat{b}_1 + \mathbf{V}_{E1} + \mathbf{V}_{D1}\big)\cdot\hat{r}\frac{\partial f_0}{\partial r} + ev_\parallel E_\parallel\frac{\partial f_0}{\partial w} + \Big(e\mathbf{V}_{D0}\cdot\mathbf{E} + \mu\frac{\partial B_1}{\partial t}\Big)\frac{\partial f_0}{\partial w} \tag{3}$$

Where $\omega_B = ck_\perp T/eBL_B$. The new terms on the right hand side are tedious and a work in progress. We do see however that the new term on the left hand side will provide coupling to L_{12} and thus be an MTM drive.

7.2 Criteria for MTMs at the pick up coils

Here is an estimate of the resulting radial magnetic fluctuations at the edge due to pedestal MTMs. The goal is to compare this estimate with radial magnetic fluctuation data from Bdot probes at the edge. A realistic computation is of course very complicated and would involve nonlinear physics. This is just a back of the envelope calculation.

The radial heat transport due to radial magnetic fluctuations (parallel streaming) is given below.

$$(q_\parallel)_r = \kappa_\parallel\hat{r}\cdot\hat{b}\big(\hat{b}\cdot\nabla T_e\big) = \kappa_\parallel\left(\frac{\delta B_r}{B_0}\right)^2\frac{\partial T_e}{\partial x}$$

Here $\kappa_\parallel$ is given by

$$\kappa_\parallel = 0.38 \frac{(T_e)^{5/2}}{m_e^{1/2} e^4 \ln \Lambda} = 1.5 \times 10^{49} T_e^{5/2}$$

We can solve for the radial magnetic fluctuations.

$$\left(\frac{\delta B_r}{B_0}\right)^2 = \frac{(q_\parallel)_r}{\kappa_\parallel \partial_x T_e}$$

Numerical values for the right hand side are experimentally known. We can assume that this parallel streaming heat transport accounts for roughly 30 percent of the total heat balance. This will give us an order of magnitude estimate of the fluctuation magnitude.

7.2.1 Radial decay of the eigenfunction

The tearing mode away from the rational surfaces will decay away. Should this decay be accounted for? For low mode number MTMs the $A_\parallel$ eigenfunction decays roughly as $\big((a-r_0)/x_e\big)^2$. Where x_e is the resonant electron length scale $x_e = \omega/(k'_\parallel v_e)$, a is the minor radius, and r_0 is the location of the rational surface.

Thus a correction can be made to the above estimates by multiplying by $\big((a-r_0)/x_e\big)^2$.

Another decaying features of is for high mode number MTMs. These high mode number MTMs could attach to decaying $\exp -k_y|x|$ solutions, and thus the mode width would be estimated by $1/k_y$.

References

[1] Guttenfelder, Walter, et al. "Gyrokinetic prediction of microstability and transport in NSTX H-mode pedestals." Bulletin of the American Physical Society 66 (2021).

[2] Larakers, "Microtearing modes in the tokamak pedestal" University of Texas at Austin PhD Dissertation (2021).

[3] Larakers, J. L., Curie, M., Hatch, D. R., Hazeltine, R. D., & Mahajan, S. M. (2021). Global Theory of Microtearing Modes in the Tokamak Pedestal. Physical Review Letters, 126(22), 225001. https://doi.org/10.1103/PhysRevLett.126.225001

[4] Drake, J. F., Antonsen, T. M., Hassam, A. B., & Gladd, N. T. (1983). Stabilization of the tearing mode in high-temperature plasma. Physics of Fluids, 26(9), 2509–2528. https://doi.org/10.1063/1.864441

[5] Hatch, D. R., Kotschenreuther, M., Mahajan, S. M., Pueschel, M. J., Michoski, C., Merlo, G., Hassan, E., Field, A. R., Frassinetti, L., Giroud,

C., Hillesheim, J. C., Maggi, C. F., Von Thun, C. P., Roach, C. M., Saarelma, S., Jarema, D., & Jenko, F. (2021). Microtearing modes as the source of magnetic fluctuations in the JET pedestal. Nuclear Fusion, 61(3). https://doi.org/10.1088/1741-4326/abd21a

[6] Curie, M. T., Larakers, J. L., Hatch, D. R., Nelson, A. O., Diallo, A., Hassan, E., Guttenfelder, W., Halfmoon, M., Kotschenreuther, M., Hazeltine, R. D., Mahajan, S. M., Groebner, R. J., Chen, J., Perez von Thun, C., Frassinetti, L., Saarelma, S., Giroud, C., & Tennery, M. M. (2022). A survey of pedestal magnetic fluctuations using gyrokinetics and a global reduced model for microtearing stability. Physics of Plasmas, 29(4), 042503. https://doi.org/10.1063/5.0084842

[7] Maingi, R., Osborne, T. H., Bell, M. G., Bell, R. E., Boyle, D. P., Canik, J. M., Diallo, A., Kaita, R., Kaye, S. M., Kugel, H. W., Leblanc, B. P., Sabbagh, S. A., Skinner, C. H., & Soukhanovskii, V. A. (2015). Dependence of recycling and edge profiles on lithium evaporation in high triangularity, high performance NSTX H-mode discharges. Journal of Nuclear Materials, 463, 1134–1137. https://doi.org/10.1016/j.jnucmat.2014.10.084